



Designing Special Nonmetallic Superalkalis Based on a Cage-like Adamanzane Complexant

Ya-Ling Ye¹, Kai-Yun Pan¹, Bi-Lian Ni¹ and Wei-Ming Sun^{1,2*}

¹Fujian Key Laboratory of Drug Target Discovery and Structural and Functional Research, The School of Pharmacy, Fujian Medical University, Fuzhou, China, ²School of Chemistry and Materials Science, University of Science and Technology of China, Hefei, China

OPEN ACCESS

Edited by:

Sugata Chowdhury,
National Institute of Standards and
Technology (NIST), United States

Reviewed by:

Gourhari Jana,
University of California, Irvine,
United States
Santanab Giri,
Haldia Institute of Technology, India

*Correspondence:

Wei-Ming Sun
sunwm@fjmu.edu.cn

Specialty section:

This article was submitted to
Physical Chemistry and Chemical
Physics,
a section of the journal
Frontiers in Chemistry

Received: 12 January 2022

Accepted: 25 February 2022

Published: 14 March 2022

Citation:

Ye Y-L, Pan K-Y, Ni B-L and Sun W-M
(2022) Designing Special Nonmetallic
Superalkalis Based on a Cage-like
Adamanzane Complexant.
Front. Chem. 10:853160.
doi: 10.3389/fchem.2022.853160

In this study, to examine the possibility of using cage-like complexants to design nonmetallic superalkalis, a series of $X@3^6\text{adz}$ ($X = \text{H, B, C, N, O, F, and Si}$) complexes have been constructed and investigated by embedding nonmetallic atoms into the 3^6adamanzane (3^6adz) complexant. Although X atoms possess very high ionization energies, these resulting $X@3^6\text{adz}$ complexes possess low adiabatic ionization energies (AIEs) of 0.78–5.28 eV. In particular, the adiabatic ionization energies (AIEs) of $X@3^6\text{adz}$ ($X = \text{H, B, C, N, and Si}$) are even lower than the ionization energy (3.89 eV) of Cs atoms, and thus, can be classified as novel nonmetallic superalkalis. Moreover, due to the existence of diffuse excess electrons in $\text{B}@3^6\text{adz}$, this complex not only possesses pretty low AIE of 2.16 eV but also exhibits a remarkably large first hyperpolarizability (β_0) of 1.35×10^6 au, indicating that it can also be considered as a new kind of nonlinear optical molecule. As a result, this study provides an effective approach to achieve new metal-free species with an excellent reducing capability by utilizing the cage-like organic complexants as building blocks.

Keywords: superalkali, adamanzane, superatom, nonlinear optics, reducing matters

INTRODUCTION

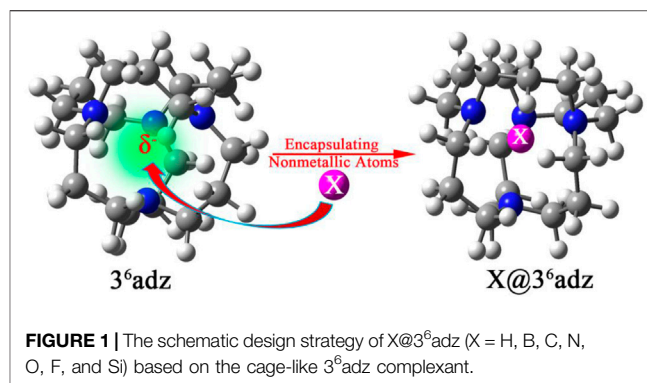
Reducing agents with low ionization energies (IEs) play a crucial role in chemical synthesis. As is well-known, alkali metal atoms possess the lowest ionization energies (5.39–3.89 eV) (Lide, 2003) among all the elements in the periodic table. However, it is reported that a class of extraordinary compounds possesses even lower IEs than those of alkali metal atoms. Such species were termed “superalkalis” by Gutsev and Boldyrev (1982). Initially, superalkalis were designed by decorating an electronegative central atom with alkali-metal ligands, such as FLi_2 , OLi_3 , and NLi_4 following the formula ML_{k+1} (L is an alkali-metal atom and M is an electronegative atom of valency k). In ML_{k+1} , one more alkali metal atom will bring an extra valence electron for the electronic shell of M according to the octet rule. Consequently, such an ML_{k+1} complex has a great tendency to lose the extra valence electron and thus possess strong reducibility (Sun and Wu, 2019).

Owing to their excellent reducing ability, superalkalis can be used to synthesize unusual charge-transfer salts (Zintl and Morawietz, 1938; Jansen, 1976) with the counterpart possessing relatively low electron affinity and activate stable CO_2 and N_2 molecules (Park and Meloni, 2017; Zhao et al., 2017; Park and Meloni, 2018; Sun et al., 2019; Sikorska and Gaston, 2020) to produce high-value products (Zhang et al., 2021a; Zhang et al., 2021b). In particular, as a special subset of superatom (Reveles et al., 2009; Luo and Castleman, 2014), superalkalis can behave as alkali metal atoms and

maintain their structural and electronic integrities when assembled into extended nanostructures (Reber et al., 2007). Hence, they offer an exciting prospect of serving as building blocks for nanomaterials with highly tunable properties (Jena and Sun 2018), such as supersalts (Giri et al., 2014), hydrogen storage materials (Merino et al., 2012), noble-gas-trapping agents (Pan et al., 2013), superbases (Srivastava and Misra, 2015), and nonlinear optical materials (Sun et al., 2014a; Sun et al., 2014b; Sun et al., 2016b; Sun et al., 2016c; Sun et al., 2018a).

In view of the great importance of superalkalis in chemistry, various superalkalis have been theoretically (Tong et al., 2009; Tong et al., 2011, Tong et al., 2012a, Tong et al., 2012b; Hou et al., 2013; Liu et al., 2014; Sun et al., 2013; Sun et al., 2016a; Giri et al., 2016; Zhao et al., 2017; Sun et al., 2018b; Sun et al., 2019; Park and Meloni, 2018; Sun and Wu, 2019; Tkachenko et al., 2019; Sikorska and Gaston, 2020) and experimentally (Lievens et al., 1999; Yokoyama et al., 2000, 2001; Hou and Wang, 2020) characterized in the past decades. To date, conventional mononuclear ML_{k+1} superalkalis have been expanded to dinuclear (Tong et al., 2009; Tong et al., 2011) and polynuclear (Tong et al., 2012a; Tong et al., 2012b; Liu et al., 2014) superalkalis, aromatic superalkalis (Sun et al., 2013), Zintl-ion-based superalkalis (Giri et al., 2016; Sun et al., 2018b), hyperalkalis (Sun et al., 2016a), alkali-metal complexes (Tkachenko et al., 2019), and so on. More importantly, some alkali-metal-free superalkalis (Hou et al., 2014; Liu et al., 2016), particularly nonmetallic superalkalis (Hou et al., 2013; Srivastava, 2019a; Srivastava, 2019b), have been proposed in recent years. For example, Hou et al. (2013) designed a class of $M_2H_{2n+1}^+$ ($M = F, O, N, C$ for $n = 1, 2, 3, 4$, respectively) superalkali cations by using hydrogen atoms as ligands. Following a similar rule, the other two series of nonmetallic superalkali cations, namely, $F_nH_{n+1}^+$ ($n = 1-10$) and $C_xH_{4x+1}^+$ ($x = 1-5$), have been proposed by Srivastava (2019a, 2019b). These achievements demonstrate that the potential of designing superalkalis of new type is limitless and thereby motivate us to create more diverse superalkali species by using different rules and ligands to further enrich the superalkali family.

More recently, Tkachenko et al. (2019) reported the record low ionization potentials (1.70–1.52 eV) of alkali metal complexes with crown ethers and cryptands and defined them as superalkali species. In fact, such alkali metal complexes were previously named as electrides, a special kind of ionic solids with trapped electrons serving as anions (Dye, 2009). Hence, this work first built a bridge between superalkalis and electrides. However, it is known that crown ethers and cryptands are prone to be cleaved at the C-O bonds (Redko et al., 2002). Fortunately, analogous complexants, such as adamanzane (adz) (Redko et al., 2002) and aza-cage (aza222) (Kim et al., 1999) with only C-N linkages and no amine hydrogens are considerably stable to synthesize the crystalline salts, including alkalides (Kim et al., 1999; Redko et al., 2002) and electrides (Redko et al., 2005) at room temperature. Hence, it is highly expected that such complexants could also be used as excellent building blocks to design and synthesize new superalkalis.



To verify this hypothesis, the $3^6adamanzane$ (3^6adz) has been chosen as a representative to design a series of $X@3^6adz$ ($X = H, B, C, N, O, F,$ and Si) by encapsulating nonmetallic atoms into the cavity of this cage-like complexant in this work (see **Figure 1**). The 3^6adz complexant is composed of tricyclic tetra-amines with aliphatic chains (Springborg, 2003), which has been used to synthesize a stable alkali $[H@3^6adz]^+Na^-$ (Redko et al., 2002). In this complexant, all the lone pairs of 4 N atoms direct toward the center of the cage (see **Supplementary Figure S1**). Under the repulsion of the lone pairs of N atoms, the outmost valence electrons of X are destabilized to different degrees, leading to the obvious rise of HOMO level of $X@3^6adz$ as compared with the isolated 3^6adz complexant. As a result, these proposed complexes exhibit extraordinarily low AIE values of 0.78–5.28 eV although X atoms possess very high ionization energies (IEs) of 8.15–17.42 eV (Lide, 2003). In particular, the $B@3^6adz$ complex also has the potential to serve as new nonlinear optical (NLO) molecule with a remarkably large first hyperpolarizability of 1.35×10^6 au because the valence electron of boron atom is pushed out of cage to form diffuse excess electrons. We hope that this work will not only provide new nonmetallic members for the superatom family, but will also open the door to design strong reducing matters by embedding nonmetallic atoms into the various cage-like complexants.

COMPUTATIONAL DETAILS

In this work, all the calculations were carried out by using the coulomb-attenuated hybrid exchange-correlation functional (CAM-B3LYP) (Tawada et al., 2004; Yanai et al., 2004), which has been reported to be capable of providing not only the molecular geometries close to the experimentally observed structures but also the (hyper)polarizabilities close to those of the coupled cluster calculations (Limacher et al., 2009). Hence, this method has been widely used to calculate the (hyper)polarizabilities of NLO molecules in the previous works (Sun et al., 2014a; Sun et al., 2014b, Sun et al., 2016c). Also, a method test has also been carried out by sampling $B@3^6adz$ (see **Supplementary Table S1**) to verify the reliability of this method in calculating the properties of such systems.

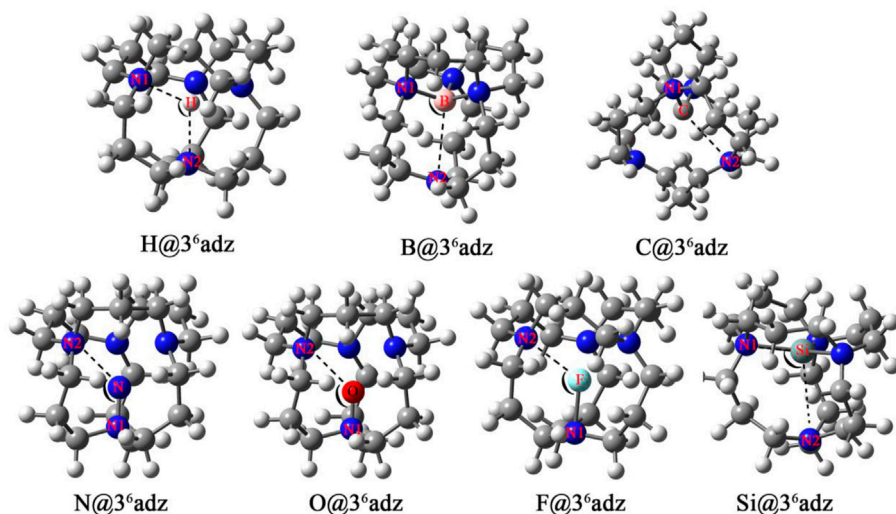


FIGURE 2 | Optimized geometric structures of $X@3^6adz$ ($X = H, B, C, N, O, F,$ and Si) compounds.

From **Supplementary Table S1**, it is found that CAM-B3LYP gives approximately equal VIE and β_0 to those obtained by several other functionals, which indicates that this method is reliable for these studied systems. Hence, all the optimized geometric structures of the studied species with real frequencies were obtained under the CAM-B3LYP/6-31+G(d) level. Based on the optimized structures, the single-point energies, nature population analysis (NPA) charges, and static electric properties were calculated at the CAM-B3LYP/6-311++G (d, p) level.

In this work, the vertical ionization energies (VIEs) of $X@3^6adz$ ($X = H, B, C, N, O, F,$ and Si) were calculated as the energy difference between the optimized neutral complex and the cation in the geometry of the neutral complex, while their adiabatic ionization energies (AIEs) are defined as the energy difference between the neutral and cationic complex at their respective optimized structures. In addition, the TD-M06-2X calculations were performed to obtain the transition energies and oscillator strengths of the crucial excited states as well as the difference of the dipole moments between the ground state and crucial excited state of $X@3^6adz$ by using the 6-311++G (d, p) basis set. Herein, the dipole moments (μ_0), polarizabilities (α_0), and first hyperpolarizabilities (β_0) are defined as follows,

$$\mu_0 = (\mu_x^2 + \mu_y^2 + \mu_z^2)^{1/2} \quad (1)$$

$$\alpha_0 = \frac{1}{3} (\alpha_{xx} + \alpha_{yy} + \alpha_{zz}) \quad (2)$$

$$\beta_0 = (\beta_x^2 + \beta_y^2 + \beta_z^2)^{1/2} \quad (3)$$

where $\beta_i = \frac{1}{3} \sum (\beta_{ijj} + \beta_{jji} + \beta_{jii})$, $i, j = \{x, y, z\}$.

All the above calculations were performed by using the GAUSSIAN 16 program package (Frisch et al., 2016). The dimensional plots of the molecular structures were generated with the GaussView program (Dennington et al., 2016).

TABLE 1 | Symmetry point group, the lowest vibrational frequencies ν_1 (in cm^{-1}), the bond lengths of X-N1 and X-N2 bonds (d_{X-N1} and d_{X-N2} , in Å), $\angle N1-X-N2$ angle (in deg) of $X@3^6adz$ ($X = H, B, C, N, O, F,$ and Si) compounds.

Species	Symmetry	ν_1	d_{X-N1}	d_{X-N2}	$\angle N1-X-N2$
H@3 ⁶ adz	S ₄	69	2.11	2.11	113.5
B@3 ⁶ adz	C ₁	91	1.66	3.02	105.9
C@3 ⁶ adz	C ₂	102	1.52	2.97	108.4
N@3 ⁶ adz	C ₁	48	1.41	2.58	120.3
O@3 ⁶ adz	C ₁	72	1.34	2.59	125.1
F@3 ⁶ adz	C ₁	61	1.87	2.41	123.7
Si@3 ⁶ adz	C ₁	76	2.06	3.22	102.0

RESULTS AND DISCUSSION

Initially, seven $X@3^6adz$ ($X = H, B, C, N, O, F,$ and Si) compounds have been constructed by encapsulating one X atom into a 3^6adz cage. After optimization, the geometric structures of $X@3^6adz$ are illustrated in **Figure 2**, while the corresponding cations are plotted in **Supplementary Figure S2**. Moreover, selected structural parameters of these resulting $X@3^6adz$ compounds are summarized in **Table 1**.

As shown in **Figure 1**, 3^6adz is a cage-like complexant with S₄ symmetry. From **Figure 2**, it is observed that the geometric integrity of 3^6adz cage is well-preserved in these $X@3^6adz$ compounds. However, the geometric symmetries of these compounds are lowered to C₁ and C₂, except for H@3⁶adz, which maintains the S₄ symmetry of 3^6adz . To be specific, the encapsulated hydrogen atom located at the central position of 3^6adz in H@3⁶adz, yields the newly formed N-H bonds of 2.11 Å and $\angle N1-H-N2$ of 113.5°. As for B@3⁶adz, the boron atom tends to bind with 3 N atoms of the complexant, forming 3 N-B bonds of 1.63 Å ~ 1.66 Å, while the distance between the uncombined N and B atoms is as long as 3.02 Å. The C@3⁶adz complex possesses a C₂-symmetric structure, where the introduced

TABLE 2 | Adiabatic ionization energies (AIEs, in eV), vertical ionization energies (VIEs, in eV), HOMO and LUMO energy levels (in eV), and the HOMO–LUMO gaps of 3^6adz and $X@3^6\text{adz}$ ($X = \text{H, B, C, N, O, F,}$ and Si) compounds.

Species	AIE	VIE	HOMO	LUMO	Gap(eV)
3^6adz	6.56	6.80	-6.49	-0.38	6.12
$\text{H}@3^6\text{adz}$	0.78	3.83	-3.49	0.36	3.86
$\text{B}@3^6\text{adz}$	2.16	2.18	-1.81	-0.01	1.80
$\text{C}@3^6\text{adz}$	2.72	3.01	-3.08	0.10	3.18
$\text{N}@3^6\text{adz}$	3.15	5.72	-4.48	0.19	4.67
$\text{O}@3^6\text{adz}$	5.28	5.86	-5.65	0.18	5.83
$\text{F}@3^6\text{adz}$	4.92	6.38	-5.87	-0.13	5.73
$\text{Si}@3^6\text{adz}$	1.79	2.73	-2.61	0.26	2.87

carbon atom prefers to bind with 2 N atoms of 3^6adz by forming two N–C bonds of 1.52 Å. Differently, the more electronegative N, O, and F atoms are linked to only 1 N atom of the cage complexant *via* N–N, N–O, and N–F bonds of 1.41, 1.34, and 1.87 Å, respectively, generating the very similar structures of $X@3^6\text{adz}$ ($X = \text{N, O,}$ and F). Similar to $\text{B}@3^6\text{adz}$, the introduced silicon atom tends to bind with 3 N atoms of complexant *via* 3 N–Si bonds of 2.06–2.35 Å in $\text{Si}@3^6\text{adz}$.

By turning to the cations of $X@3^6\text{adz}$, it is found that only the optimized structure of $[\text{B}@3^6\text{adz}]^+$ cation almost coincides with the geometry of the corresponding neutral one (see **Supplementary Figure S2**). For instance, the critical geometric parameters of $d_{\text{B-N}_1}$, $d_{\text{B-N}_2}$, and $\angle\text{N}_1\text{-B-N}_2$ are hardly changed after one electron is lost from $\text{B}@3^6\text{adz}$. However, for the rest of $X@3^6\text{adz}$ ($X = \text{H, C, N, O, F,}$ and Si), quite different geometries of cationic and neutral complexes were found. For instance, the H^+ is attached to 1 N atom of the complexant in the resulting $[\text{H}@3^6\text{adz}]^+$, while the doped N atom turns to combine with 2 N atoms of 3^6adz in $[\text{N}@3^6\text{adz}]^+$ and Si atom almost moves to the center of the cage in $[\text{Si}@3^6\text{adz}]^+$. The geometry of $\text{C}@3^6\text{adz}$ is distorted from C_2 symmetry to C_1 with the changes of 0.29 Å for the C–N2 bond and 7.3° for $\angle\text{N}_1\text{-C-N}_2$. As for $[\text{F}@3^6\text{adz}]^+$, the N–F bond is shortened from 1.87 Å to 1.38 Å because the introduced F atom further loses 0.333e (see **Supplementary Table S1**) and thus tends to bind more tightly with the N atom of the complexant. Also, as shown in **Table 2**, the difference in the geometry can also be reflected by the difference of 0.29–3.06 eV between the vertical ionization energies (VIEs) and adiabatic ionization energies (AIEs) of these $X@3^6\text{adz}$ ($X = \text{H, C, N, O, F,}$ and Si) species.

More interestingly, as shown in **Table 2**, extraordinarily low AIE values of 0.78–5.28 eV were found for all the studied $X@3^6\text{adz}$ ($X = \text{H, B, C, N, O, F,}$ and Si) complexes, although X atoms possess very high ionization energies (IEs) of 8.15–17.42 eV (Lide, 2003). Such low AIE values of $X@3^6\text{adz}$ are not only lower than that of 6.56 eV for the 3^6adz complexant but also significantly lower than that of 5.39 eV (Lide, 2003) for lithium atom. In particular, the AIE values of $\text{H}@3^6\text{adz}$ (0.78 eV), $\text{B}@3^6\text{adz}$ (2.16 eV), $\text{C}@3^6\text{adz}$ (2.72 eV), $\text{N}@3^6\text{adz}$ (3.15 eV), and $\text{Si}@3^6\text{adz}$ (1.79 eV) are even lower than the IE of 3.89 eV (Lide, 2003) for Cs atoms. Hence, these compounds should be classified as novel nonmetallic superalkalis.

How to understand the low IE values of such $X@3^6\text{adz}$ complexes? We can find some clues from the frontier molecular orbital analysis. From **Figure 3**, a clear inverse correlation between the VIE values and HOMO levels of these studied compounds can be observed, that is, the higher the HOMO level is, the lower the VIE is. This is reasonable considering the fact that the valence electrons on the higher HOMOs are easier to be ionized. To be specific, all the HOMO energies (−1.81 ~ −5.87 eV) of $X@3^6\text{adz}$ are much higher than that of −6.49 eV for 3^6adz , because of the repulsion between the lone pairs of N atoms and the outmost valence electrons of X, resulting in the lower VIEs (2.18–6.38 eV) than that (6.80 eV) of 3^6adz . In particular, $\text{B}@3^6\text{adz}$ exhibits the highest HOMO level of −1.81 eV, and thus possesses the lowest VIE of 2.18 eV among these $X@3^6\text{adz}$ complexes. This is because that the valence electron of embedded boron atom is pushed out of the cage by the lone pairs of N atoms of the complexant, forming a electronegative-like molecule $[\text{B}^+@3^6\text{adz}](\text{e}^-)$ with obvious diffuse electrons in the HOMO of $\text{B}@3^6\text{adz}$ (see **Supplementary Figure S3**). Thus, the existence of diffuse excess electrons in its high-lying HOMO level results in the high reducibility of this $\text{B}@3^6\text{adz}$ complex.

Differently, as shown in **Supplementary Figure S3**, the valence electrons are accommodated into the HOMOs mainly composed of the 1s atomic orbital of embedded hydrogen atom in $\text{H}@3^6\text{adz}$, and the *np* orbitals of C and Si atoms in $X@3^6\text{adz}$ ($X = \text{C}$ and Si), which show obvious antibonding character with respect to the central atom–complexant interaction. Such antibonding HOMOs destabilize the neutral structures of $X@3^6\text{adz}$ ($X = \text{H, C,}$ and Si) and result in their low VIE values (Gutsev and Boldyrev, 1987; Tkachenko et al., 2019). Hence, these 3 species also have quite low VIE values of 2.73–3.83 eV. However, it should be mentioned that the VIEs of 5.72–6.38 eV for $X@3^6\text{adz}$ ($X = \text{N, O,}$ and F) are larger than that of 5.39 eV for Li atom, although their HOMOs also possess obvious

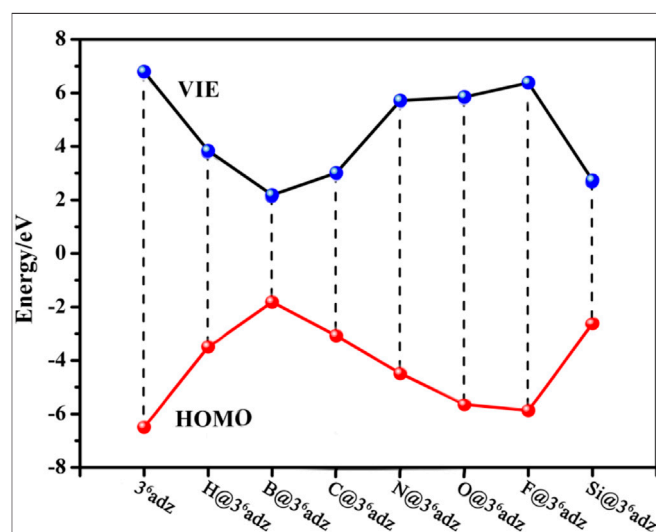


FIGURE 3 | The relationship between the VIE values and HOMO levels of $X@3^6\text{adz}$ ($X = \text{H, B, C, N, O, F,}$ and Si) compounds.

TABLE 3 | Calculated dipole moments (μ_0 , in au), polarizabilities (α_0 , in au), first hyperpolarizabilities (β_0 , in au), transition energies (ΔE , in eV), oscillator strength (f_0), and the difference in the dipole moments ($\Delta\mu$, in Debye) between the ground and crucial excited states of 3^6adz and $X@3^6\text{adz}$ ($X = \text{H, B, C, N, O, F, and Si}$) compounds.

Species	μ_0	α_0	β_0	ΔE	f_0	$\Delta\mu$
3^6adz	0.000	240	0	5.64	0.100	1.113
$\text{H}@3^6\text{adz}$	0.000	253	0	5.03	0.044	0.001
$\text{B}@3^6\text{adz}$	3.326	1,599	1.35×10^6	0.40	0.121	6.428
$\text{C}@3^6\text{adz}$	2.074	278	4.05×10^3	2.25	0.064	2.854
$\text{N}@3^6\text{adz}$	1.471	257	2.84×10^2	4.67	0.033	0.495
$\text{O}@3^6\text{adz}$	1.558	249	6.84×10^2	5.40	0.059	1.801
$\text{F}@3^6\text{adz}$	1.142	255	2.43×10^2	3.52	0.093	0.544
$\text{Si}@3^6\text{adz}$	0.773	354	1.95×10^4	1.84	0.040	5.663

antibonding character. This is attributed to the larger electronegativities of N, O, and F atoms than H, C, and Si atoms, which hinders the ionization of the valence electrons on their np orbitals in the HOMOs of $X@3^6\text{adz}$ ($X = \text{N, O, and F}$).

On the other hand, the difference between the VIE and AIE values are also related to the different electron distribution in the HOMOs of $X@3^6\text{adz}$. To be specific, the geometric structure of $\text{B}@3^6\text{adz}$ is hardly changed after its diffuse excess electron of HOMO is lost, resulting in its nearly equal VIE (2.18 eV) and AIE (2.16 eV) values. However, the destabilization of antibonding HOMOs for the neutral $X@3^6\text{adz}$ ($X = \text{H, C, and Si}$) complexes drives the embedded X atom to lose nearly one valence electron ($0.667e \sim 0.867e$, as shown in **Supplementary Table S1**), forming relatively stable $[X@3^6\text{adz}]^+$ cations. After losing one electron, the formed X^+ ion changes its interaction mode with the cage complexant, which leads to the large structural distortion and considerable difference between the VIE and AIE values of $X@3^6\text{adz}$ ($X = \text{H, C, and Si}$). Note that the AIE of $\text{H}@3^6\text{adz}$ is as low as 0.78 eV because the formed $[\text{H}@3^6\text{adz}]^+$ is very stable and has been identified in various synthesized ionic compounds, such as $[\text{H}@3^6\text{adz}]^+\text{X}^-$ ($X = \text{Cl, Br, I, and Na}$) (Kim et al., 1994; Springborg et al., 1996; Redko et al., 2002).

Finally, considering the diffuse excess electron in the HOMO of $\text{B}@3^6\text{adz}$, it is highly expected that this superalkali also exhibits considerable nonlinear optical (NLO) response. Thus, the static electric properties of these studied $X@3^6\text{adz}$ compounds and 3^6adz complexant were calculated and listed in **Table 3**. It is observed that $\text{B}@3^6\text{adz}$ has the largest dipole moment (3.326 au) and polarizability (1,599 au) among these $X@3^6\text{adz}$ complexes because of the existence of diffuse electrons in the HOMO of this superalkali. In particular, the first hyperpolarizability (β_0) of $\text{B}@3^6\text{adz}$ is as large as 1.35×10^6 au, which is significantly larger than those of the reported superalkalis and superalkali-based NLO materials, such as the aromatic organometallic superalkali $\text{Au}_3(\text{Py})_3$ (3.74×10^4 au) (Parida et al., 2018), superalkali-based alkalide $\text{Li}_3\text{O}^+(\text{calix}[4]\text{pyrrole})\text{M}^-$ ($M = \text{Li, Na, and K}$) (1.18×10^4 – 3.33×10^4 au) (Sun et al., 2014a), and superalkali-based electride $\text{Li}_3\text{O}@\text{Al}_{12}\text{N}_{12}$ (8.73×10^5 au) (Sun et al., 2016b), indicating that this

proposed superalkali species can indeed be considered as a new kind of NLO molecule of high performance.

To understand the eminently large β_0 value of $\text{B}@3^6\text{adz}$, we focus our attention on the simple two-level model (Oudar, 1977; Oudar and Chemla, 1977),

$$\beta_0 \propto \frac{\Delta\mu \cdot f_0}{\Delta E^3} \quad (4)$$

where ΔE , f_0 , and $\Delta\mu$ are the transition energy, oscillator strength, and the difference in the dipole moment between the ground state and crucial excited state, respectively. According to this two-level expression, β_0 is proportional to f_0 and $\Delta\mu$, while is inversely proportional to the cube of ΔE , and therefore, the transition energy is considered to be the decisive factor in the first hyperpolarizability (Sun et al., 2014a,b, 2016b,c). Hence, the ΔE , f_0 , and $\Delta\mu$ values of the crucial excited states with the largest oscillator strength of 3^6adz and $X@3^6\text{adz}$ are summarized in **Table 3**. It is noted that $\text{B}@3^6\text{adz}$ possesses extremely smaller ΔE and much larger f_0 and $\Delta\mu$ values than those of other $X@3^6\text{adz}$ ($X = \text{H, C, N, O, F, and Si}$) compounds, which rationalizes its largest β_0 value among these studied $X@3^6\text{adz}$ species. In addition, the proposed $\text{C}@3^6\text{adz}$ and $\text{Si}@3^6\text{adz}$ superalkalis also show considerable β_0 values of 4.05×10^3 au and 1.95×10^4 au, respectively, because of their relatively smaller ΔE values and larger $\Delta\mu$ values.

CONCLUSION

By using 3^6adamanzane (3^6adz) as a complexant, a series of $X@3^6\text{adz}$ ($X = \text{H, B, C, N, O, F, and Si}$) compounds were constructed and studied based on the density functional theory. It is interesting to find that the $X@3^6\text{adz}$ ($X = \text{H, B, C, N, and Si}$) complexes possess lower AIE values than the IE of Cs atoms though the X atoms and 3^6adz possess very high IE values. Thereby, they can be regarded as a new kind of nonmetallic superalkalis. In particular, different from other complexes, the low IE of $\text{B}@3^6\text{adz}$ is derived from the diffuse excess electron formed by the repulsion between the valence electron of the embedded boron atom and lone pairs of N atoms of the complexant. Due to the existence of diffuse electrons, this superalkali also possesses a remarkably large β_0 of 1.35×10^6 au, which can serve as a new kind of NLO molecule. Hence, it is highly hoped that the theoretical design and characterization of these nonmetallic superalkali species could provide meaningful references to further design novel reducing matters or NLO materials by using such cage-like molecules as complexants.

DATA AVAILABILITY STATEMENT

The original contributions presented in the study are included in the article/**Supplementary Material**, further inquiries can be directed to the corresponding author.

AUTHOR CONTRIBUTIONS

All authors listed have made a substantial, direct and intellectual contribution to the work and approved it for publication.

FUNDING

This work was supported by the Natural Science Foundation of Fujian Province (2021J01682) and the National Natural Science Foundation of China (21603032).

REFERENCES

- Dennington, R. D., Keith, T. A., and Millam, J. M. (2016). *GaussView, Version 6*. Shawnee Mission, KS: Semicem Inc.
- D. R. Lide (Editor) (2003). *CRC Handbook of Chemistry and Physics* (Boca Raton, Florida: CRC Press).
- Dye, J. L. (2009). Electrides: Early Examples of Quantum Confinement. *Acc. Chem. Res.* 42, 1564–1572. doi:10.1021/ar9000857
- Frisch, M. J., Trucks, G. W., Schlegel, H. B., Scuseria, G. E., Robb, M. A., Cheeseman, J. R., et al. (2016). *Gaussian 16, Revision A.03*. Wallingford CT, USA: Gaussian, Inc.
- Giri, S., Behera, S., and Jena, P. (2014). Superalkalis and Superhalogens as Building Blocks of Supersalts. *J. Phys. Chem. A*. 118 (3), 638–645. doi:10.1021/jp4115095
- Giri, S., Reddy, G. N., and Jena, P. (2016). Organo-Zintl Clusters [P7R4]: A New Class of Superalkalis. *J. Phys. Chem. Lett.* 7, 800–805. doi:10.1021/acs.jpcclett.5b02892
- Gutsev, G. L., and Boldyrev, A. I. (1982). DVM X α Calculations on the Electronic Structure of "superalkali" Cations. *Chem. Phys. Lett.* 92, 262–266. doi:10.1016/0009-2614(82)80272-8
- Gutsev, G. L., and Boldyrev, A. I. (1987). The Electronic Structure of Superhalogens and Superalkalis. *Russ. Chem. Rev.* 56 (6), 519–531. doi:10.1070/rc1987v056n06abeh003287
- Hou, G.-L., and Wang, X.-B. (2020). Potassium Iodide Cluster Based Superhalogens and Superalkalis: Theoretical Calculations and Experimental Confirmation. *Chem. Phys. Lett.* 741, 137094. doi:10.1016/j.cplett.2020.137094
- Hou, N., Li, Y., Wu, D., and Li, Z.-R. (2013). Do Nonmetallic Superalkali Cations Exist? *Chem. Phys. Lett.* 575, 32–35. doi:10.1016/j.cplett.2013.05.014
- Hou, N., Wu, D., Li, Y., and Li, Z.-R. (2014). Lower the Electron Affinity by Halogenation: an Unusual Strategy to Design Superalkali Cations. *J. Am. Chem. Soc.* 136 (7), 2921–2927. doi:10.1021/ja411755t
- Jansen, M. (1976). Na³NO₃-kein Orthonitrit. *Angew. Chem. Int. Ed.* 88, 411. doi:10.1002/ange.19760881205
- Jena, P., and Sun, Q. (2018). Super Atomic Clusters: Design Rules and Potential for Building Blocks of Materials. *Chem. Rev.* 118 (11), 5755–5870. doi:10.1021/acs.chemrev.7b00524
- Kim, J., Ichimura, A. S., Huang, R. H., Redko, M., Phillips, R. C., and Jackson, J. E. (1999). Crystalline Salts of Na and K (Alkalides) that Are Stable at Room Temperature. *J. Am. Chem. Soc.* 121, 10666–10667. doi:10.1021/ja992667v
- Kim, R. D. H., Wilson, M., and Haseltine, H. (1994). Simple Preparations of Tricyclic Orthoamides and Macrocyclic Triamines. *Synth. Commun.* 24 (21), 3109–3114. doi:10.1080/00397919408011324
- Lievens, P., Thoen, P., Bouckaert, S., Bouwen, W., Vanhoutte, F., Weidele, H., et al. (1999). Ionization Potentials of Li_nO (2 ≤ n ≤ 70) Clusters: Experiment and Theory. *J. Chem. Phys.* 110 (21), 10316. doi:10.1063/1.478965
- Limacher, P. A., Mikkelsen, K. V., and Lüthi, H. P. (2009). On the Accurate Calculation of Polarizabilities and Second Hyperpolarizabilities of Polyacetylene Oligomer Chains Using the CAM-B3lyp Density Functional. *J. Chem. Phys.* 130 (19), 194114. doi:10.1063/1.3139023
- Liu, J. Y., Wu, D., Sun, W. M., Li, Y., and Li, Z. R. (2014). Trivalent Acid Radical-Centered YLi₄⁺ (Y = PO₄, AsO₄, VO₄) Cations: New Polynuclear Species Designed to Enrich the Superalkali Family. *Dalton Trans.* 43 (48), 18066–18073. doi:10.1039/c4dt02347a

ACKNOWLEDGMENTS

We thank the National Supercomputing Center in Shenzhen for providing computational resources.

SUPPLEMENTARY MATERIAL

The Supplementary Material for this article can be found online at: <https://www.frontiersin.org/articles/10.3389/fchem.2022.853160/full#supplementary-material>

- Liu, J. Y., Xi, Y. J., Li, Y., Li, S. Y., Wu, D., and Li, Z. R. (2016). Does Alkaline-Earth-Metal-Based Superalkali Exist? *J. Phys. Chem. A*. 120 (51), 10281–10288. doi:10.1021/acs.jpca.6b10555
- Luo, Z., and Castleman, A. W. (2014). Special and General Superatoms. *Acc. Chem. Res.* 47 (10), 2931–2940. doi:10.1021/ar5001583
- Merino, G., Chattaraj, P. M., and Pan, S. (2012). Hydrogen Trapping Potential of Some Li-Doped Star-like Clusters and Super-alkali Systems. *Phys. Chem. Chem. Phys.* 14, 10345–10350. doi:10.1039/c2cp40794a
- Oudar, J. L., and Chemla, D. S. (1977). Hyperpolarizabilities of the Nitroanilines and Their Relations to the Excited State Dipole Moment. *J. Chem. Phys.* 66 (6), 2664. doi:10.1063/1.434213
- Oudar, J. L. (1977). Optical Nonlinearities of Conjugated Molecules. Stilbene Derivatives and Highly Polar Aromatic Compounds. *J. Chem. Phys.* 67 (2), 446. doi:10.1063/1.434888
- Pan, S., Contreras, M., Romero, J., Reyes, A., Chattaraj, P. K., and Merino, G. (2013). C₅Li₇⁺ and O₂Li₅⁺ as Noble-Gas-Trapping Agents. *Chem. Eur. J.* 19 (7), 2322–2329. doi:10.1002/chem.201203245
- Parida, R., Reddy, G. N., Ganguly, A., Roymahapatra, G., Chakraborty, A., and Giri, S. (2018). On the Making of Aromatic Organometallic Superalkali Complexes. *Chem. Commun.* 54 (31), 3903–3906. doi:10.1039/c8cc01170b
- Park, H., and Meloni, G. (2018). Activation of Dinitrogen with a Superalkali Species, Li₃F₂. *ChemPhysChem* 19 (3), 256–260. doi:10.1002/cphc.201701232
- Park, H., and Meloni, G. (2017). Reduction of Carbon Dioxide with a Superalkali. *Dalton Trans.* 46 (35), 11942–11949. doi:10.1039/c7dt02331f
- Reber, A. C., Khanna, S. N., and Castleman, A. W. (2007). Superatom Compounds, Clusters, and Assemblies: Ultra Alkali Motifs and Architectures. *J. Am. Chem. Soc.* 129, 10189–10194. doi:10.1021/ja071647n
- Redko, M. Y., Jackson, J. E., Huang, R. H., and Dye, J. L. (2005). Design and Synthesis of a Thermally Stable Organic Electride. *J. Am. Chem. Soc.* 127, 12416–12422. doi:10.1021/ja053216f
- Redko, M. Y., Vlassa, M., Jackson, J. E., Misiolek, A. W., Huang, R. H., and Dye, J. L. (2002). Inverse Sodium Hydride⁺: A Crystalline Salt that Contains H and Na-. *J. Am. Chem. Soc.* 124, 5928–5929. doi:10.1021/ja025655+
- Reveles, J. U., Clayborne, P. A., Reber, A. C., Khanna, S. N., Pradhan, K., Sen, P., et al. (2009). Designer Magnetic Superatoms. *Nat. Chem.* 1 (4), 310–315. doi:10.1038/nchem.249
- Sikorska, C., and Gaston, N. (2020). N₄Mg₆M (M = Li, Na, K) Superalkalis for CO₂ Activation. *J. Chem. Phys.* 153, 144301. doi:10.1063/5.0025545
- Springborg, J. (2003). Adamanzanes-Bi- and Tricyclic Tetraamines and Their Coordination Compounds. *Dalton Trans.* (9), 1653–1665. doi:10.1039/b300510k
- Springborg, J., Pretzmann, U., and Olsen, C. E. (1996). An Inert Proton Coordinated inside the Tetrahedral Cage [3⁵]Adamanzane. Synthesis of the inside Monoprotonated Amine 1,5,9,13-Tetraazatricyclo[7.7.3.3^{5,13}]docosane. *Acta Chem. Scand. A*. 50, 294–298. doi:10.3891/acta.chem.scand.50-0294
- Srivastava, A. K. (2019a). Ab Initio investigations on Non-metallic Chain-Shaped F_nH_{n+1}⁺ Series of Superalkali Cations. *Chem. Phys. Lett.* 721, 7–11. doi:10.1016/j.cplett.2019.02.021
- Srivastava, A. K. (2019b). C_xH_{4x+1}⁺ (X = 1–5): a Unique Series of Organic Superalkali Cations. *Mol. Phys.*, 1–7.
- Srivastava, A. K., and Misra, N. (2015). Superalkali-hydroxides as Strong Bases and Superbases. *New J. Chem.* 39 (9), 6787–6790. doi:10.1039/c5nj01259g

- Sun, W.-M., Li, C.-Y., Kang, J., Wu, D., Li, Y., Ni, B.-L., et al. (2018a). Superatom Compounds under Oriented External Electric Fields: Simultaneously Enhanced Bond Energies and Nonlinear Optical Responses. *J. Phys. Chem. C* 122 (14), 7867–7876. doi:10.1021/acs.jpcc.8b01896
- Sun, W.-M., Li, X.-H., Li, Y., Liu, J.-Y., Wu, D., Li, C.-Y., et al. (2016a). On the Feasibility of Designing Hyperalkali Cations Using Superalkali Clusters as Ligands. *J. Chem. Phys.* 145 (19), 194303. doi:10.1063/1.4967461
- Sun, W.-M., Li, X.-H., Wu, D., Li, Y., He, H.-M., Li, Z.-R., et al. (2016b). A Theoretical Study on Superalkali-Doped Nanocages: Unique Inorganic Electrides with High Stability, Deep-Ultraviolet Transparency, and Considerable Nonlinear Optical Response. *Dalton Trans.* 45 (17), 7500–7509. doi:10.1039/c6dt00342g
- Sun, W.-M., Li, Y., Wu, D., and Li, Z.-R. (2013). Designing Aromatic Superatoms. *J. Phys. Chem. C* 117 (46), 24618–24624. doi:10.1021/jp408810e
- Sun, W.-M., Wu, D., Kang, J., Li, C.-Y., Chen, J.-H., Li, Y., et al. (2018b). Decorating Zintl Polyanions with Alkali Metal Cations: A Novel Strategy to Design Superatom Cations with Low Electron Affinity. *J. Alloys Compd.* 740 (5), 400–405. doi:10.1016/j.jallcom.2017.12.075
- Sun, W.-M., Zhang, X.-L., Pan, K.-Y., Chen, J.-H., Wu, D., Li, C.-Y., et al. (2019). On the Possibility of Using the Jellium Model as a Guide to Design Bimetallic Superalkali Cations. *Chem. Eur. J.* 25 (17), 4358–4366. doi:10.1002/chem.201806194
- Sun, W. M., Fan, L. T., Li, Y., Liu, J. Y., Wu, D., and Li, Z. R. (2014a). On the Potential Application of Superalkali Clusters in Designing Novel Alkalides with Large Nonlinear Optical Properties. *Inorg. Chem.* 53 (12), 6170–6178. doi:10.1021/ic500655s
- Sun, W. M., Li, Y., Li, X. H., Wu, D., He, H. M., Li, C. Y., et al. (2016c). Stability and Nonlinear Optical Response of Alkalides that Contain a Completely Encapsulated Superalkali Cluster. *Chemphyschem* 17 (17), 2672–2678. doi:10.1002/cphc.201600389
- Sun, W. M., Wu, D., Li, Y., and Li, Z. R. (2014b). Theoretical Study on Superalkali (Li_3) in Ammonia: Novel Alkalides with Considerably Large First Hyperpolarizabilities. *Dalton Trans.* 43 (2), 486–494. doi:10.1039/c3dt51559a
- Sun, W. M., and Wu, D. (2019). Recent Progress on the Design, Characterization, and Application of Superalkalis. *Chem. Eur. J.* 25 (41), 9568–9579. doi:10.1002/chem.201901460
- Tawada, Y., Tsuneda, T., Yanagisawa, S., Yanai, T., and Hirao, K. (2004). A Long-Range-Corrected Time-dependent Density Functional Theory. *J. Chem. Phys.* 120, 8425–8433. doi:10.1063/1.1688752
- Tkachenko, N. V., Sun, Z. M., and Boldyrev, A. I. (2019). Record Low Ionization Potentials of Alkali Metal Complexes with Crown Ethers and Cryptands. *Chemphyschem* 20 (16), 2060–2062. doi:10.1002/cphc.201900422
- Tong, J., Li, Y., Wu, D., Li, Z.-R., and Huang, X.-R. (2011). Ab Initio Investigation on a New Class of Binuclear Superalkali Cations $\text{M}_2\text{Li}_{2k+1}^+$ (F_2Li_3^+ , O_2Li_5^+ , N_2Li_7^+ , and C_2Li_9^+). *J. Phys. Chem. A.* 115 (10), 2041–2046. doi:10.1021/jp110417z
- Tong, J., Li, Y., Wu, D., Li, Z. R., and Huang, X. R. (2009). Low Ionization Potentials of Binuclear Superalkali B_2Li_{11} . *J. Chem. Phys.* 131 (16), 164307. doi:10.1063/1.3254835
- Tong, J., Li, Y., Wu, D., and Wu, Z.-J. (2012a). Theoretical Study on Polynuclear Superalkali Cations with Various Functional Groups as the Central Core. *Inorg. Chem.* 51 (11), 6081–6088. doi:10.1021/ic202675j
- Tong, J., Wu, Z., Li, Y., and Wu, D. (2012b). Prediction and Characterization of Novel Polynuclear Superalkali Cations. *Dalton Trans.* 42, 577–584. doi:10.1039/c2dt31429k
- Yanai, T., Tew, D. P., and Handy, N. C. (2004). A New Hybrid Exchange–Correlation Functional Using the Coulomb-Attenuating Method (CAM-B3lyp). *Chem. Phys. Lett.* 393 (1–3), 51–57. doi:10.1016/j.cplett.2004.06.011
- Yokoyama, K., Haketa, N., Tanaka, H., Furukawa, K., and Kudo, H. (2000). Ionization Energies of Hyperlithiated Li_2F Molecule and $\text{Li}_n\text{F}_{n-1}$ ($N=3, 4$) Clusters. *Chem. Phys. Lett.* 330, 339–346. doi:10.1016/s0009-2614(00)01109-x
- Yokoyama, K., Tanaka, H., and Kudo, H. (2001). Structure of Hyperlithiated Li_3O and Evidence for Electronomers. *J. Phys. Chem. A.* 105, 4312–4315. doi:10.1021/jp0037450
- Zhang, X.-L., Ye, Y.-L., Zhang, L., Li, X.-H., Yu, D., Chen, J.-H., et al. (2021a). Designing an Alkali-metal-like Superatom Ca_3B for Ambient Nitrogen Reduction to Ammonia. *Phys. Chem. Chem. Phys.* 23 (34), 18908–18915. doi:10.1039/d1cp01533h
- Zhang, X.-L., Zhang, L., Ye, Y.-L., Li, X.-H., Ni, B.-L., Li, Y., et al. (2021b). On the Role of Alkali-metal-like Superatom Al_{12}P in Reduction and Conversion of Carbon Dioxide. *Chem. Eur. J.* 27 (3), 1039–1045. doi:10.1002/chem.202003733
- Zhao, T., Wang, Q., and Jena, P. (2017). Rational Design of Super-alkalis and Their Role in CO_2 Activation. *Nanoscale* 9 (15), 4891–4897. doi:10.1039/c7nr00227k
- Zintl, E., and Morawietz, W. (1938). Orthosalze von Sauerstoffsäuren. *Z. Anorg. Allg. Chem.* 236, 372–410. doi:10.1002/zaac.19382360134

Conflict of Interest: The authors declare that the research was conducted in the absence of any commercial or financial relationships that could be construed as a potential conflict of interest.

Publisher's Note: All claims expressed in this article are solely those of the authors and do not necessarily represent those of their affiliated organizations, or those of the publisher, the editors, and the reviewers. Any product that may be evaluated in this article, or claim that may be made by its manufacturer, is not guaranteed or endorsed by the publisher.

Copyright © 2022 Ye, Pan, Ni and Sun. This is an open-access article distributed under the terms of the Creative Commons Attribution License (CC BY). The use, distribution or reproduction in other forums is permitted, provided the original author(s) and the copyright owner(s) are credited and that the original publication in this journal is cited, in accordance with accepted academic practice. No use, distribution or reproduction is permitted which does not comply with these terms.